Article

Effect of Steel Fiber Content on Shear Behavior of Reinforced Expanded-Shale Lightweight Concrete Beams with Stirrups

Changyong Li [1,*], Minglei Zhao [2,*], Xiaoyan Zhang [1], Jie Li [2], Xiaoke Li [1] and Mingshuang Zhao [1]

1   International Joint Research Lab for Eco-Building Materials and Engineering of Henan,
     School of Civil Engineering and Communications, North China University of Water Resources and Electric
     Power, Zhengzhou 450045, China; zxyanzi@ncwu.edu.cn (X.Z.); lixk@ncwu.edu.cn (X.L.);
     zhaoms@stu.ncwu.edu.cn (M.Z.)
2   School of Engineering, RMIT University, Melbourne, VIC 3003, Australia; jie.li@rmit.edu.au
*   Correspondence: lichang@ncwu.edu.cn (C.L.); s3339909@student.rmit.edu.au (M.Z.);
     Tel.: +86-371-69127388 (C.L.)

Abstract: To determine the validity of steel fiber reinforced expanded-shale lightweight concrete (SFRELC) applied in structures, the shear behavior of SFRELC structural components needs to be understood. In this paper, four-point bending tests were carried out on reinforced SFRELC beams with stirrups and a varying volume fraction of steel fiber from 0.4% to 1.6%. The shear cracking force, shear crack width and distribution pattern, mid-span deflection, and failure modes of test beams were recorded. Results indicate that the shear failure modes of reinforced SFRELC beams with stirrups were modified from brittle to ductile and could be transferred to the flexure mode with the increasing volume fraction of steel fiber. The coupling of steel fibers with stirrups contributed to the shear cracking force and the shear capacity provided by the SFRELC, and it improved the distribution of shear cracks. At the limit loading level of beams in building structures at serviceability, the maximum width of shear cracks could be controlled within 0.3 mm and 0.2 mm with the volume fraction of steel fiber increased from 0.4% to 0.8%. Finally, the formulas are proposed for the prediction of shear-cracking force, shear crack width, and shear capacity of reinforced SFRELC beams with stirrups.

Keywords: steel fiber reinforced expanded-shale lightweight concrete (SFRELC); reinforced SFRELC beam; stirrups; volume fraction of steel fiber; shear cracking; shear crack width; shear capacity

1. Introduction

In the construction of high-rise buildings and large span spatial structures as well as long span bridges, the self-weight of the structure is a key issue which should be of concern. This promotes the development of lightweight aggregate concrete. Due to the different resources and manufactured methods, many kinds of lightweight aggregates are market supplied. The material widely used for structural concrete in China is the sintered expanded-shales. After a series experimental studies, a high-performance steel fiber reinforced expanded-shale lightweight concrete (SFRELC) is produced. The sintered expanded-shale and the ceramsite sand are used for the aggregates of SFRELC to realize the lightweight itself. On the previous studies, SFRELC has the characteristics of structural material with desirable mechanical properties [1,2], volume stability [3], and good dura-bility [4]. Moreover, the bond of a steel bar with SFRELC is reliable [5]. This provides the foundation of SFRELC applied in structural engineering.

The studies on the flexural behavior of reinforced SFRELC beams under static concen-trated loads indicated that the cracking moment, flexural stiffness, and bearing capacity as well as ductility are effectively promoted with the increasing volume fraction of steel fibers from 0.4% to 1.6%, and the crack growth is confined with decreased spacing and width [6–8]. A fatigue life of reinforced SFRELC superposed beams with ductile failure

mode was prolonged by preventing fatigue fracture of longitudinal tensile rebar and reducing crack growth, and the failure could be expected with the trend curves of fatigue flexural stiffness [9]. By the experimental study on shear-cracking force and shear crack extension, mid-span deflection, shear failure mode, and shear capacity, the effective enhancement of steel fibers was confirmed on the shear behavior of reinforced SFRELC beams without stirrups; however, the brittle failure could not be prevented with the rupture of expanded shales along diagonal cracks [10]. This indicates the efficiency of steel fiber to increase the behavior of reinforced SFRELC beams in tension.

Currently, few studies were reported on the shear behavior of steel fiber reinforced lightweight aggregate concrete (SFRLAC) beams with stirrups. Nes and Øverli [11] studied the structural behaviors of layered beams with SFRLAC and conventional concrete, and the results show that the stirrups might be reduced due to the ductility of SFRLAC in tension increased by steel fibers; the shear capacity of test beams increased with the increased content of steel fiber and depended on the distribution and orientation of steel fibers. Jiao et al. [12] investigated the shear behavior of reinforced SFRLAC beams, and the results indicate that accompanied with the rupture of coarse lightweight aggregate on the failure sections, the failure of test beams changed from shear to flexural shear with the increasing amount of steel fiber; the shear capacity provided by stirrups and the shear ductility of test beams could be increased by the presence of steel fiber due to the enhanced bond property of stirrups with SFRLAC.

In view of the above research studies, the interaction of steel fiber with stirrups needs to be identified. However, there is lack of research on the shear behavior of reinforced SFRLAC beams, let alone the shear behavior of reinforced SFRELC beams. In this condition, we may learn from the shear functions of steel fiber and stirrups in steel fiber reinforced concrete (SFRC) beams based on the similar shear mechanisms. A number of experimental studies indicate that steel fibers have potential advantages when used to supplement or replace stirrups in reinforced SFRC beams, which can effectively improve the shear behavior in combination with stirrups. Zhao et al. [13–15] indicate that the improvement of steel fibers on shear-cracking force and shear capacity of reinforced SFRC beams is consistent to that of the tensile strength of SFRC, which was independent of the stirrups. Meanwhile, the distribution of diagonal cracks was affected by the interaction of steel fibers and stirrups. Stirrups in a small spacing made the uniform width of diagonal cracks, while steel fibers limited the extension of these cracks. Researchers exhibit that [16–19] the inclusion of steel fibers in adequate content can change the failure mechanism from brittle shear into ductile flexure. This confirms the possibility of using steel fiber reinforcement instead of increasing the stirrups amount to achieve analogous performance for reinforced SFRC beams. Similarly, steel fiber reinforcement can be used with a combination of reduced stirrups to satisfy the shear capacity and ductility of reinforced SFRC beams [19–23]. As a result, replacing minimum stirrups was feasible by a certain amount of steel fibers in the condition of reinforced SFRC beams in flexural failure [24–27]. On the other hand, the minimum stirrups play a better role of controlling shear cracks than steel fibers in terms of more diagonal cracks with small width at failure, and they effectively mitigate the size effect of depth on the shear capacity of reinforced SFRC beams [28,29]. A study performed by di Prisco and Romero [30] shows that in combination with stirrups, the hybrid fibers are quite substantial to the diagonal shear of thin-webbed reinforced concrete beams. Moreover, a certain amount of steel fiber trends are more effective than stirrups for the control of shear cracks on reinforced SFRC beams with different shear span to depth ratios, while the contribution of steel fibers on the shear capacity of reinforced SFRC beams depends on the situations of different ratios of stirrups [31–34].

2. Research Significance

Due to the shear behavior of reinforced concrete beams closely connected to the properties of concrete, the attention should be noted on the shear behavior related to aggregate type, which affects the strength of concrete, the dowel action of longitudinal

reinforcement, the interlocking action of aggregates along the cracked section, and the bond–slip of stirrups with concrete [5,10,35–37]. Obviously, current study is insufficient on the shear behavior of reinforced SFRELC beams, and it cannot be applied as a reliable design consideration. In this paper, an experimental research study was carried out to fill in the research gap on the shear behavior of reinforced SFRELC beams with stirrups. Ten test beams were designed to pronounced shear failure. Test results are directly compared to the previous study of reinforced SFRELC beams without stirrups [10] and evaluated with the specifications of current design codes [37–39]. Finally, the predictive formulas for the shear-cracking force, shear capacity, and shear crack width of reinforced SFRELC beams are proposed considering the featured strengthening effect of steel fibers with stirrups.

3. Experimental Work

3.1. Production of SFRELC

Grade 52.5 ordinary silicate cement, sintering expanded shale, ceramsite sand, poly-carboxylic acid super-plasticizer, milling steel fiber, and tap water were used for SFRELC. The properties of cement were 27.4% water requirement of normal consistency, 51.7 MPa of compressive strength, and 9.2 MPa of tensile strength at 28 days. The sintered expanded shale was continuous grading with a maximum particle size of 20 mm, bulk and particle densities of 800 and 1274 kg/m^3, cylinder compressive strength of 5.0 MPa, and water absorption for 1 h of 6.1%. The ceramsite sand was the by-product of sintered expanded shale in continuous grading with particle size of 1.6–5 mm, a fineness modulus of 3.56, bulk and particle densities of 946 and 1659 kg/m^3, and water absorption for 1 h of 9.0%. The steel fiber was of milling type in length l_f = 36 mm and equivalent diameter d_f = 1.35 mm, the aspect ratio l_f/d_f = 27.1. The mix water was the tap water of Zhengzhou city, China.

The mix proportion of SFRELC was primarily designed by the absolute volume method and adjusted to keep the slump of fresh SFRELC at (120 ± 20) mm [7,10,37,40]. The volume fraction v_f of steel fiber was changed to 0%, 0.4%, 0.8%, 1.2%, and 1.6%. The fiber factor λ_f = 27.1v_f. The additional water for pre-wetting the sintered expanded-shale and ceramic sand was computed with 1 h water absorptions.

The fresh SFRELC was mixed by a single-horizontal-shaft mixer. The expanded shale and ceramic sand with the additional water was firstly pre-wetted in the mixer for 1 h. Then, the cement and half dosage of the mix water were added and mixed for 30 s. The super-plasticizer and the residual mix water were added during the mixing, and the steel fiber was sprinkled into the mixer and mixed for 3 min [3–7,10].

According to the specification of China code JG/T472 [40], the standard specimens for the test of strength of SFRELC were fabricated and cured at the same condition of test beams. The splitting tensile strength f_{ft} of SFRELC was tested by three cubes of 150 mm, and the axial compressive strength f_{fc} was tested by three prisms of 150 mm × 150 mm × 300 mm. The tested values are presented in Table 1.

Table 1. Dimension, influencing factor of test beams, and main tested results.

Identifier	b (mm)	h_0 (mm)	vf (%)	Strength of SFRELC (MPa)		Computed Shear Force (kN)	
				ffc	fft	$V_{u(1)}$	$V_{u(4)}$
LC2.5-0.25-0a	150	362	0	36.4	2.80	143	177
LC2.5-0.25-0b	155	362	0	36.4	2.80	145	178
LC2.5-0.25-0.4a	150	362	0.4	42.4	3.04	151	179
LC2.5-0.25-0.4b	150	362	0.4	42.4	3.04	151	179
LC2.5-0.25-0.8a	155	362	0.8	49.2	3.17	157	182
LC2.5-0.25-0.8b	155	362	0.8	49.2	3.17	157	182
LC2.5-0.25-1.2a	150	362	1.2	51.6	3.31	160	182
LC2.5-0.25-1.2b	150	362	1.2	51.6	3.31	160	182
LC2.5-0.25-1.6a	150	362	1.6	52.3	3.62	170	182
LC2.5-0.25-1.6b	155	364	1.6	52.3	3.62	171	182

3.2. Design and Fabrication of Test Beams

The reinforced SFRELC beams were designed to have a pronounced shear behavior with the popular rectangular section. As found in previous study [10], the shear capacity of reinforced SFRELC beams without web reinforcements depends on the shear span to depth ratio, the longitudinal reinforcement ratio, and the tensile strength of SFRELC. The effects of steel fiber focused on the bearing capacity of SFRELC in the shear and compression zone, the interlock among aggregates along sides of diagonal cracks, and the dowel action of longitudinal tensile rebar. In the designing of test beams with stirrups, the shear capacity V_u was supposed as the independent contribution of stirrups with the composition of the beams without web reinforcements [37–39], that is,

$$V_u = V_{fcu} + V_{sv}. \tag{1}$$

The shear resistance V_{fcu} provided by SFRELC was computed by formula [10],

$$V_{fcu} = \frac{0.115 + 0.192\lambda + 28.7\rho}{\lambda - 0.6} f_{ft}bh_0. \tag{2}$$

The shear resistance V_s provided by stirrups was computed by formula [38,39],

$$V_{sv} = \rho_{sv}f_{yv}bh_0. \tag{3}$$

In the formulas, b is the sectional width; h_0 is the sectional effective depth, $h_0 = h - c_s - d/2$, h is the sectional depth, c_s is the concrete cover; f_{ft} is the tensile strength of SFRELC; ρ is the ratio of longitudinal rebars, $\rho = A_s/bh_0$, taken $\rho = 3.0\%$ when $\rho \geq 3.0\%$; A_s is the cross-sectional area of longitudinal tensile rebars; λ is the shear span to depth ratio, $\lambda = a/h_0$, taken $\lambda = 4$ when $\lambda \geq 4$, a is the shear span; ρ_{sv} is the ratio of stirrups, $\rho_{sv} = A_{sv}/bs$; A_{sv} is the cross-sectional area of stirrups; s is the spacing of stirrups; f_{yv} is the yield strength of stirrups.

Meanwhile, the flexural capacity of test beams was designed by using the formulas provided in previous study [7],

$$M_{fu} = f_yA_s\left(h_0 - \frac{x}{2}\right) + f_{ftu}bx_t\left(h - \frac{x}{2} - \frac{x_t}{2}\right) \tag{4}$$

$$f_{fc}bx = f_yA_s + f_{ftu}bx_t \tag{5}$$

$$x_t = h - \frac{x}{0.75} \tag{6}$$

$$f_{ftu} = 1.86\lambda_f f_t \tag{7}$$

where M_{fu} is the moment capacity of the reinforced SFRELC beam; x is the compressive depth of the cross-section; x_t is the equal tensile depth of the cross-section; f_y is the yield strength of longitudinal tensile rebars; f_{ftu} is the equal tensile strength of SFRELC in the tensile zone of the cross-section, f_t is the tensile strength of the SFRELC matrix; and λ_f is the fiber factor, i.e., the product of v_f and l_f/d_f.

Based on above formulas, ten beams were designed; two of them identified as a/b were the same in each group, as presented in Table 1. The width b = 150 mm, the depth h = 400 mm, the length l = 3200 mm, and the span l_0 = 2900 mm. Details of the rebars in the test beams are presented in Figure 1. The longitudinal tensile rebars were two hot-rolled HRB500 ribbed rebars with diameter d = 25 mm, the concrete cover c_s = 25 mm. The constructional compression rebars were two hot-rolled HPB300 plain rebars with a diameter of 8 mm. The stirrups were the hot-rolled HPB300 plain rebar with a diameter of 6 mm.

The tensile strength of rebars was measured. The yield strength f_y = 517 MPa and the ultimate strength was 598 MPa for the hot-rolled HRB500 ribbed rebar with a diameter of

25 mm. The yield strength f_{yv} = 398 MPa and the ultimate strength was 529 MPa for the hot-rolled HPB300 plain rebar with a diameter of 6mm.
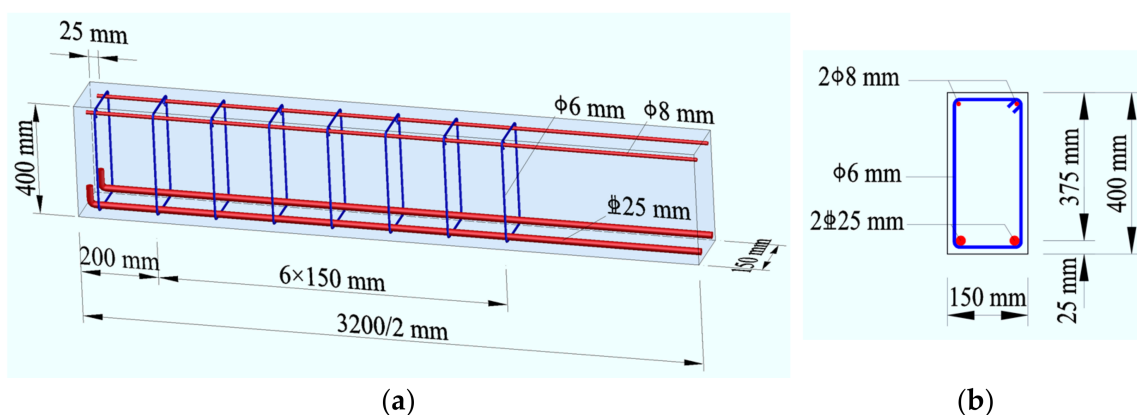

Figure 1. Layout of reinforcements in test beams: (**a**) longitudinal section; (**b**) transversal section.

The shear span to depth ratio of the test beams λ = 2.5, the shear span of test beam a = 905 mm. The spacing of stirrups s = 150 mm, the stirrups ratio ρ_{sv} = 0.25%. The measured sectional dimension, the shear force $V_{u(1)}$ computed by Formula (1), and that $V_{u(4)}$ (= M_{fu}/a) computed by Formula (4) for the test beams are also presented in Table 1. This shows that the test beams were designed to fail in shear due to $V_{u(1)}$ being less than $V_{u(4)}$.

The fresh SFRELC was cast twice into the steel form, and it was compacted with the outside vibrators fixed on the steel form. The screeding top-surface was covered by plastic film for 48 h before being demolded. After being demolded, the test beams were cured with sprayed water for 7 days and then placed in the outdoor environment before testing.

3.3. Test Method

As presented in Figure 2, the four-point bending test was carried out with the shear span a = 905 mm and the pure bending segment of 1090 mm. The beam was simply supported on the supports. A hydraulic jack fixed on a loading frame were used to exert the symmetrical concentrated loads on the top surface of the test beam by a spreader steel beam.
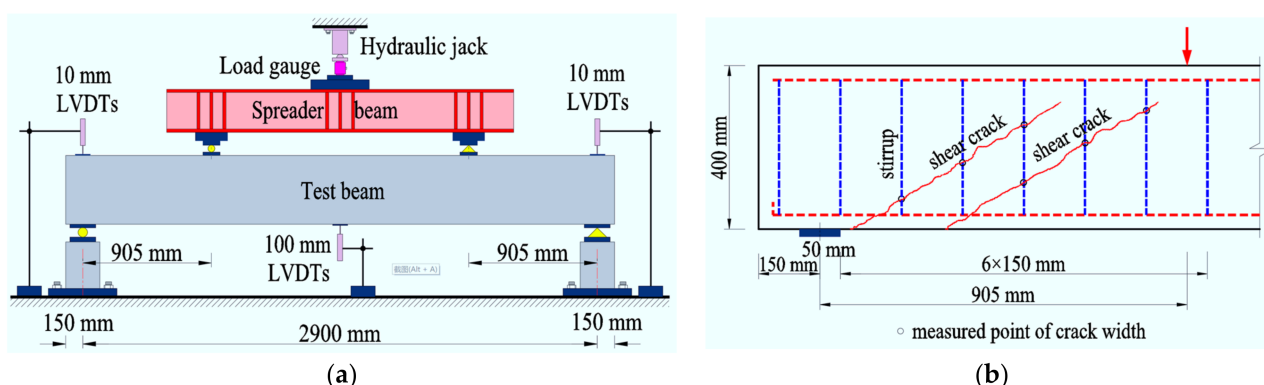

Figure 2. Test method: (**a**) testing apparatus; (**b**) measuring of shear crack width.

Load gauges were linked to the hydraulic jack to measure the values of loads. The mid-span deflection was determined by three displacement sensors (LVDTs-linear variable differential transformer) placed at the supports and mid-span section of the test beam. The width of the shear crack on the side surfaces that intersected the stirrups of the test beam

was detected with a reading microscope. The angle of the shear crack with the bottom surface of the test beam was determined as the diagonal angle of the shear crack.

4. Test Results and Analyses

4.1. Patterns of Crack Distribution and Failure

The crack distribution and failure mode of test beams are presented in Figure 3. The shear cracks appeared on the shear span after the flexural cracks appeared at the pure bending segment. This indicates that the shear-cracking resistance of the diagonal section was higher than the flexural cracking resistance of the normal section for test beams.
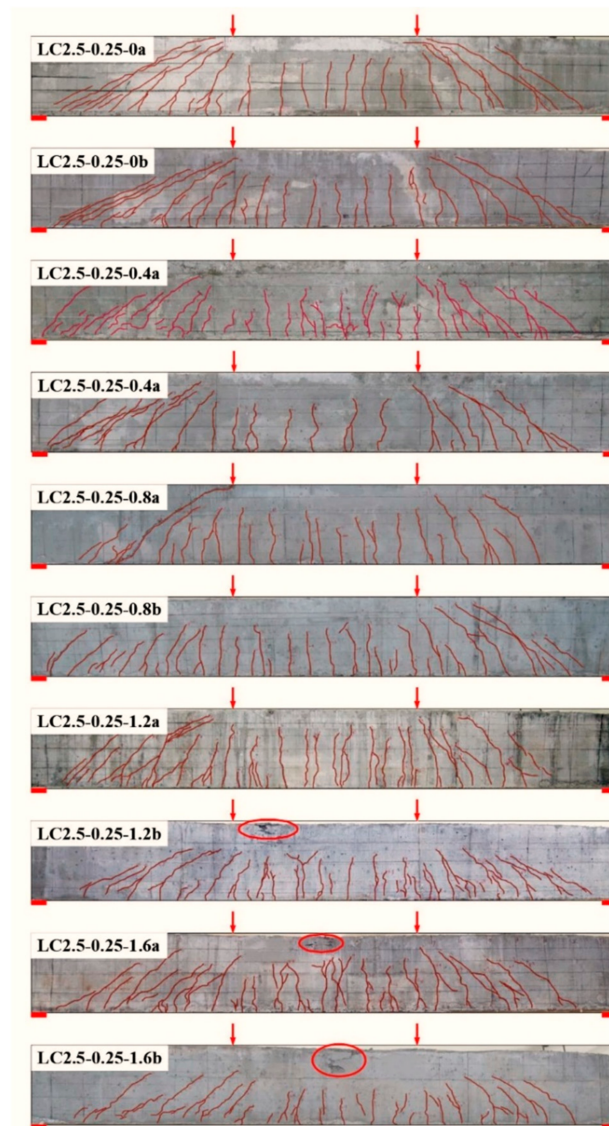

Figure 3. Crack distribution and failure mode of test beams.

For test beams LC2.5-0.25-0a/b without steel fiber reinforcement, one or two main diagonal cracks appeared on the shear span, and the shear failure with wider diagonal cracks took place. With the increasing volume fraction of steel fibers v_f, the number of shear cracks increased, the diagonal cracks slowly extended, and the diagonal angle of the main shear crack tended to be reduced slightly. Meanwhile, the shear-compression zone existed clearly with uncrack depth near loading points. The shear failure with smaller diagonal cracks took place on test beams with $v_f \leq 0.8\%$, and the failure in the shear compression

mode took place on test beam LC2.5-0.25-1.2a with $v_f = 1.2\%$. This is in keeping with the pronounced shear failure of design.

However, test beam LC2.5-0.25-1.2b with $v_f = 1.2\%$ failed in shear accompanied by flexure, and test beams LC2.5-0.25-1.2a/b with $v_f = 1.6\%$ failed in flexure. Due to the shorter diagonal cracks extended on shear span, a larger shear-compression zone was reserved near the loading points. This effectively increased the shear resistance provided by the uncracked SFRELC in shear compression. Meanwhile, the presence of stirrups confined the extension of diagonal cracks, which benefits the steel fibers bridging the diagonal cracks to transfer tensile stress. Hence, the enhancement of steel fibers on the shear capacity of reinforced SFRELC beams with stirrups was higher than that of reinforced SFRELC beams without stirrups. This led to a lower value predicted by Formula (2), which was based on the research of reinforced SFRELC beams without stirrups [10]. In this condition, the positive interaction of steel fibers and stirrups on the shear capacity of reinforced SFRELC beams should be considered.

As exhibited in Figure 4, similar changes existed for the mid-span deflection of test beams. This indicates a slight difference on the dowel action of longitudinal reinforcement. Therefore, the function of steel fibers was reflected to increase the number of shear cracks and to decrease the crack width. This enhances the interlocks of aggregates along the cracked section, and it reduces the bond–slip of stirrups with SFRELC.
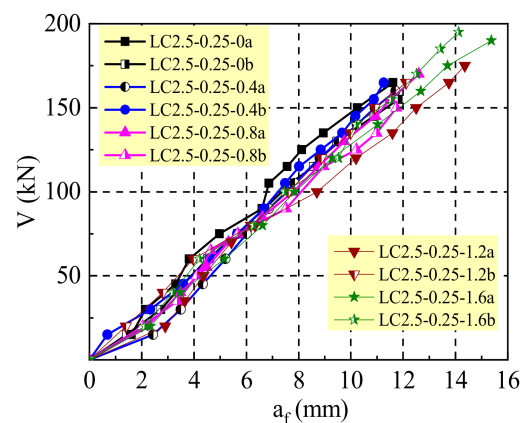

Figure 4. Mid-span deflection of test beams.

Figure 5 presents the maximum width of the main shear cracks on test beams at different loading levels V/V_u. With the increase of v_f, the shear cracking took place at an increased loading level, and the crack opened slowly with a smaller width at the same loading level after cracking. At the limit loading level of 0.74 for beams of building structures at serviceability, the maximum width of shear cracks on beams without steel fiber was close to 0.4 mm, which is controlled at normal environment; when the $v_f = 0.4\%$, the maximum width reduced to be within 0.3 mm; when the $v_f \geq 0.8\%$, the maximum width reduced to be within 0.2 mm. This provides a good adaptability of reinforced SFRELC beams in a more severe environment [38,39].

4.2. Shear-Cracking Force

The shear-cracking force V_{cr} computed by the loads corresponding to shear cracking are presented in Table 2. In this study, the shear cracking was determined as an initial inclined web crack or a shear–flexural crack was beginning to turn to the load point [10,37–39]. With the increase of v_f, the initial shear crack width tended to reduce from 0.06 mm to 0.03 mm. This exhibited that steel fibers played a role to confine the opening of shear cracks.
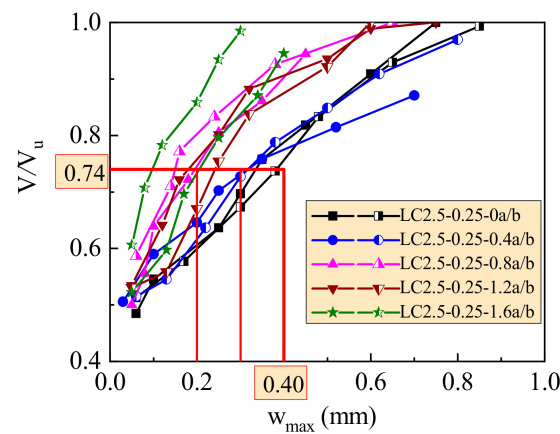
Figure 5. Shear crack widths of test beams at different loading levels.

Table 2. Test and calculation results of shear-cracking force, shear capacity, and failure mode.

Identifier	V_{cr} (kN)		Failure Pattern	V_u (kN)		
	Test	Computed		Test	Computed by Formulas (1), (3) and (10)	Computed by Formula (11)
LC2.5-0.25-0a	80	77.7	Shear	165	143	124
LC2.5-0.25-0b	80	79.8	Shear	156	145	125
LC2.5-0.25-0.4a	90	84.3	Shear	178	151	130
LC2.5-0.25-0.4b	85	84.3	Shear	165	151	130
LC2.5-0.25-0.8a	90	91.8	Shear	180	160	137
LC2.5-0.25-0.8b	95	91.8	Shear	172	160	137
LC2.5-0.25-1.2a	100	90.3	Shear	187	166	141
LC2.5-0.25-1.2b	95	90.3	Shear-flexural	179	166	141
LC2.5-0.25-1.6a	105	100.4	Flexural	201	173	147
LC2.5-0.25-1.6b	105	103.1	Flexural	198	175	149

To facilitate compressive analysis, the shear stress τ_{cr} was computed as the shear-cracking force on the unit sectional area,

$$\tau_{cr} = V_{cr}/bh_0. \tag{8}$$

As presented in Figure 6, the shear stress τ_{cr} and the tensile strength f_{ft} have linear relationships with the fiber factor λ_f. The digits 0.72 and 0.64 before λ_f in the fitness formula are the strengthening coefficients of steel fiber on τ_{cr} and f_{ft}, respectively.
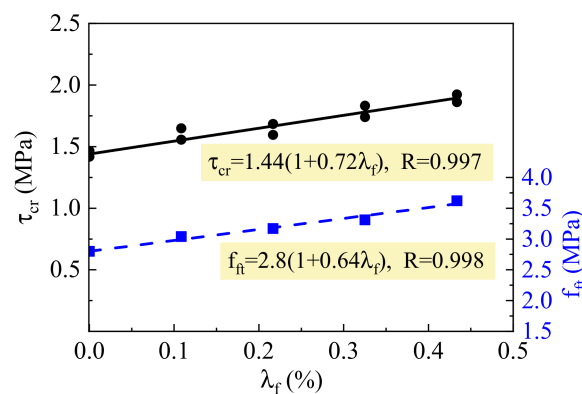

Figure 6. Changes of τ_{cr} and f_{ft} with λ_f.

Obviously, the strengthening coefficient 0.72 of τ_{cr} is greater than the 0.64 of f_{ft}. This is differing from the fact that the τ_{cr} of reinforced SFRELC beams without stirrups increased almost the same with f_{ft} [10]. Therefore, the reinforcement of steel fiber on the shear cracking resistance is not only controlled by the tensile strength of SFRELC but also improved by the stirrups due to the beneficial stress distribution of SFRELC at shear span.

To simplify the computation, the beneficial effect of stirrups on shear cracking resistance can be considered as a reliability reserve. The same formula can be used for predicting the shear-cracking force of reinforced SFRELC beams with or without web reinforcement [10],

$$V_{cr} = \left(\frac{2.45}{\lambda + 3.5} + \frac{20\rho}{\lambda + 1.1} \right) f_{ft} bh_0. \tag{9}$$

Table 2 presents the calculated values of V_{cr} by using Formula (9). Based on the statistical analysis, the average of ratios of test to calculation results is 1.034 with the coefficient of variation as 0.027. Therefore, a slightly lower value is predicted by using Formula (9).

4.3. Shear Capacity

The test peak shear force V_u computed by the peak load on test beams is summarized in Table 2. Due to the failed shear and shear-flexural patterns of test beams with $v_f = 1.2\%$, the peak shear forces of them were falling in between shear failure and flexural failure. Due to failed flexural pattern of test beams with $v_f = 1.6\%$, the peak shear forces were lower than the shear capacity.

In the premise of the shear force provided by stirrups calculated by Formula (3), the beneficial effects of stirrups can be comprehensively counted by correcting the shear force subjected by SFRELC. From Formula (1), we can obtain $V_{fcu} = V_u - V_{sv}$. Referenced to Formula (8), let $\tau_{fcu} = V_{fcu}/bh_0$. The fitted linear relationship of τ_{fcu} with λ_f is presented in Figure 7. The strengthening coefficient of steel fiber that interacted with stirrups on shear resistance provided by SFRELC is 0.78, which is greater than that of 0.64 (see Figure 6) for tensile strength of SFRELC. This reflects the coupling effect of steel fibers with stirrups on the shear capacity provided by SFRELC.
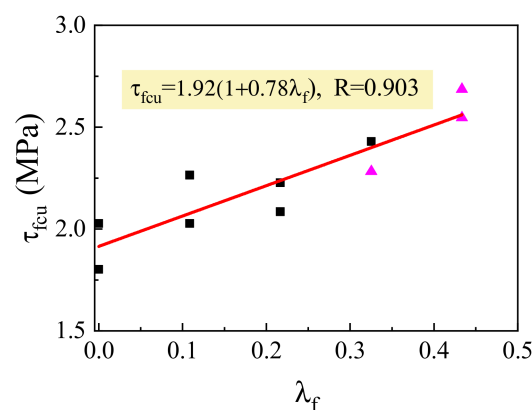

Figure 7. Changes of τ_{fcu} with λ_f.

Referencing the form $f_{ft} = f_t(1 + 0.64\lambda_f)$, Formula (2) can be transferred to be Formula (10) as follows,

$$V_{fcu} = \frac{0.115 + 0.192\lambda + 28.7\rho}{\lambda - 0.6} f_t(1 + 0.78\lambda_f) bh_0. \tag{10}$$

Referring to the design principle of shear capacity with sufficient reliability for reinforced concrete and SFRC beams specified in worldwide design codes such as CSA 23.3-04 [41], Eurocode 2 [42], ACI 318-14 [43], JGJ/T465 [39], and ACI 544.4R [44], a lower

computed shear capacity of reinforced SFRELC beams can be calculated on the basis of the design formula of lightweight-aggregate concrete beams [37],

$$V_u = \frac{1.5\beta_\rho}{\lambda + 1.0} f_t (1 + 0.78\lambda_f) bh_0 + \frac{A_{sv}f_{yv}}{s} h_0 \tag{11}$$

where $\lambda = 1$ when $\lambda < 1$, and $\lambda = 4.0$ when $\lambda > 4.0$. $\beta_\rho = 0.7 + 20\rho$.

The computed shear capacities of test beams are presented in Table 2. By using Formula (11), the shear capacities of test beams are predicted with the average reduction of 30.8%. This gives a conservative shear capacity of the reinforced SFRELC beams with stirrups.

4.4. Shear-Crack Width

To predict the shear-crack width of reinforced SFRELC beams in normal service condition, the formulas for reinforced SFRC beams are revised and expressed as follows [14],

$$w_{max} = (1 - 1.21\lambda_f) \frac{\sigma_{sv,m}}{E_{sv}} h_0 \cdot \sqrt{0.83 - 0.64\lambda h_0/l_0} \tag{12}$$

$$\sigma_{sv,m} = \frac{V - 0.9V_{cr}}{0.6\lambda\rho_{sv}bh_0} \tag{13}$$

where w_{max} is the maximum width of shear cracks intersected with stirrups; $\sigma_{sv,m}$ is the tensile stress of stirrups; E_{sv} is the modulus of elasticity of stirrups; and l_0 is the span.

Within the loading level of the normal service state, the comparison of the test and computation results of the maximum width of shear cracks is presented in Figure 8. The ratios varied from 0.346 to 1.621, the variation tended to decrease with the increasing volume fraction of steel fiber. Based on the statistical analysis, the ratio was 1.0 on average with a coefficient of variation of 0.274.
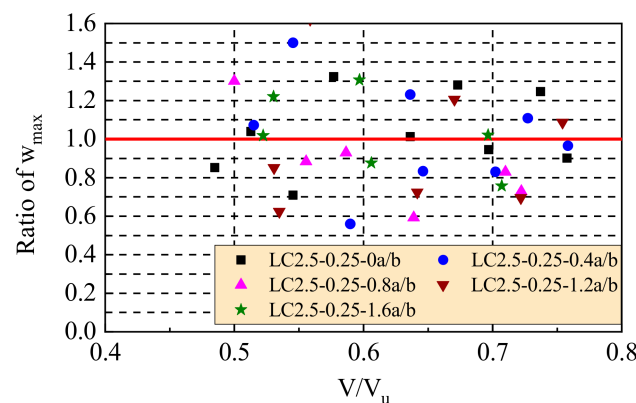

Figure 8. Comparison of test to calculation results of the maximum diagonal crack width.

Due to the randomness of shear crack extension, the width of the main diagonal cracks was affected by complex factors. It is difficult to accurately predict the width of shear cracks. Therefore, the width of shear cracks is always indirectly limited by using the design method of a conservative shear capacity [37–39]. In this study, the design shear capacity of test beams by Equation (11) was reduced by 30.8% compared with the test results. This indicates the real loading level at normal serviceability will be reduced by 30.8% from the limit loading level of 0.74; that is, 0.74/1.308 = 0.566. From Figure 5, the crack width could be strictly controlled within 0.2 mm even 0.1 mm. This provides a good condition of reinforced SFRELC beams applied in severe environment.

5. Conclusions

Based on the shear testing of reinforced SFRELC beams with stirrups, and compared with the shear behavior of reinforced SFRELC beams without stirrups in previous study, conclusions are drawn as follows:

(1) Steel fiber had a higher strengthening effect coupling with stirrups on the shear-cracking resistance of reinforced SFRELC beams. For simplifying the calculation, the beneficial effect can be neglected to provide a conservative result only considering the strengthening of steel fiber on the tensile strength of SFRELC.

(2) With the increase of steel fiber content, the shear failure could be modified with good ductility and transferred to the flexure. The stirrups improved the distribution of shear cracks with reduced spacing and width. This provided a good condition of SFRELC subjected to shear force to improve the shear capacity provided by SFRELC. Considering the effect of steel fiber reinforcement on the shear capacity of beams provided by SFRELC, the formulas are proposed for the prediction and the design of shear capacity of reinforced SFRELC beams with stirrups.

(3) With the increase of steel fiber content, the maximum width of shear cracks became smaller after shear cracking, and it extended slowly at the same loading level of test beams. The reduction of maximum width of shear cracks promoted the adaptability of reinforced SFRELC beams in a severe environment. Based on the test results, the formula for the prediction of maximum width of shear cracks is proposed.

(4) The study was limited to the changes of steel fiber content in condition of the constant shear span to depth ratio and stirrups ratio. To build a broad recognized method for the design of reinforced SFRELC beams under shear stress, many more systematical research studies need to carried out to identify the effects of multiple factors.

Author Contributions: Methodology, X.L. and J.L.; tests, data interpretation and writing—original draft, C.L., M.Z. (Minglei Zhao), X.Z. and M.Z. (Mingshuang Zhao); writing—review, M.Z. (Minglei Zhao), X.L. and J.L.; funding acquisition, X.Z. and C.L. All authors have read and agreed to the published version of the manuscript.

Institutional Review Board Statement: Not applicable.

Informed Consent Statement: Not applicable.

Data Availability Statement: Data is contained within the article.

Conflicts of Interest: The authors declare no conflict of interest.

References

1. Zhao, M.L.; Zhao, M.S.; Chen, M.H.; Li, J.; Law, D. An experimental study on strength and toughness of steel fiber reinforced expanded-shale lightweight concrete. *Constr. Build. Mater.* **2018**, *183*, 493–501. [CrossRef]
2. Zhao, M.S.; Zhang, B.; Shang, P.R.; Fu, Y. Complete Stress–Strain Curves of Self-Compacting Steel Fiber Reinforced Expanded-Shale Lightweight Concrete under Uniaxial Compression. *Materials* **2019**, *12*, 2979. [CrossRef]
3. Zhao, S.B.; Li, C.Y.; Zhao, M.S.; Zhang, X.Y. Experimental Study on Autogenous and Drying Shrinkage of Steel Fiber Reinforced Lightweight-Aggregate Concrete. *Adv. Mater. Sci. Eng.* **2016**, *2016*, 1–9. [CrossRef]
4. Zhao, M.S.; Zhang, X.Y.; Song, W.H.; Li, C.Y.; Zhao, S.B. Development of Steel Fiber-Reinforced Expanded-Shale Lightweight Concrete with High Freeze-Thaw Resistance. *Adv. Mater. Sci. Eng.* **2018**, *2018*, 1–8. [CrossRef]
5. Zhao, M.S.; Zhang, X.Y.; Yan, K.; Fei, T.; Zhao, S.B. Bond performance of deformed rebar in steel fiber reinforced lightweight-aggregate concrete affected by multi-factors. *Civ. Eng. J.* **2018**, *3*, 276–290. [CrossRef]
6. Li, C.Y.; Zhao, S.B.; Chen, H.; Gao, D.Y. Experimental study on flexural capacity of reinforced SFRFLC superposed beams. *J. Build. Struct.* **2015**, *2*, 257–264.
7. Zhao, M.S.; Li, C.Y.; Su, J.; Shang, P.R.; Zhao, S.B. Experimental study and theoretical prediction of flexural behaviors of reinforced SFRELC beams. *Constr. Build. Mater.* **2019**, *208*, 454–463. [CrossRef]

8. Li, C.Y.; Li, Q.; Li, X.K.; Zhang, X.Y.; Zhao, S.B. Elasto-plastic bending behaviors of reinforced SFRELC beams analyzed by nonlinear finite-element method. *Case Study Constr. Mater.* **2020**, *13*, e00372.

9. Qu, F.L.; Li, C.Y.; Peng, C.; Ding, X.X.; Hu, X.; Pan, L.Y. Flexural Fatigue Performance of Steel Fiber Reinforced Expanded-Shales Lightweight Concrete Superposed Beams with Initial Static-Load Cracks. *Materials* **2019**, *12*, 3261. [CrossRef]

10. Li, X.K.; Li, C.Y.; Zhao, M.L.; Yang, H.; Zhou, S.Y. Testing and prediction of shear performance for steel fiber reinforced expanded-shale lightweight concrete beams without web reinforcements. *Materials* **2019**, *12*, 1594. [CrossRef]

11. Nes, L.G.; Øverli, J.A. Structural behaviour of layered beams with fibre-reinforced LWAC and normal density concrete. *Mater. Struct.* **2015**, *49*, 689–703. [CrossRef]

12. Jiao, C.J.; Xu, B.F.; Gao, J.Y.; Wang, L. Experiments on shear resistance of steel fiber reinforced lightweight aggregate concrete beams. *J. Civ. Eng. Manag.* **2017**, *34*, 9–13.

13. Zhao, S.B.; Li, F.L.; Zhao, G.F.; Huang, C.K. Experimental research on shear cracking strength of steel fiber reinforced concrete beams. *J. Hydroelectr. Eng.* **1997**, *4*, 18–29.

14. Zhao, S.B.; Zhao, G.F.; Huang, C.K. Shear-crack width of steel fiber reinforced prestressed concrete beams. *J. Dalian Univ. Technol.* **1998**, *38*, 705–710.

15. Zhao, S.B.; Li, F.L.; Zhao, G.F.; Huang, C.K. Shear resistance of steel fiber reinforced concrete beams. *J. Basic Sci. Eng.* **1998**, *6*, 77–82.

16. Cucchiara, C.; Mendola, L.L.; Papia, M. Effectiveness of stirrups and steel fibers as shear reinforcement. *Cem. Concr. Compos.* **2004**, *26*, 777–786. [CrossRef]

17. You, Z.; Ding, Y.; Niederegger, C. Replacing stirrups of self-compacting concrete beams with steel fibers. *Trans. Tianjin Univ.* **2010**, *16*, 411–416. [CrossRef]

18. Tahenni, T.; Chemrouk, M.; Lecompte, T. Effect of steel fibers on the shear behavior of high strength concrete beams. *Constr. Build. Mater.* **2016**, *105*, 14–28. [CrossRef]

19. Ding, Y.; You, Z.; Jalali, S. The composite effect of steel fibres and stirrups on the shear behaviour of beams using self-consolidating concrete. *Eng. Struct.* **2011**, *33*, 107–117. [CrossRef]

20. Oh, B.H.; Kim, E.S.; Lim, D.H.; Yoo, S.W. Shear behaviour and shear analysis of reinforced concrete beams containing steel fibres. *Mag. Concr. Res.* **1998**, *50*, 283–291. [CrossRef]

21. Dancygier, A.N.; Savir, Z. Effects of Steel Fibers on Shear Behavior of High-Strength Reinforced Concrete Beams. *Adv. Struct. Eng.* **2011**, *14*, 745–761. [CrossRef]

22. Cucchiara, C.; Fossetti, M.; Papia, M. Steel fibre and transverse reinforcement effects on the behaviour of high strength concrete beams. *Struct. Eng. Mech.* **2012**, *42*, 551–570. [CrossRef]

23. Lim, D.; Oh, B. Experimental and theoretical investigation on the shear of steel fibre reinforced concrete beams. *Eng. Struct.* **1999**, *21*, 937–944. [CrossRef]

24. Amin, A.; Foster, S.J. Shear strength of steel fiber reinforced concrete beams with stirrups. *Eng. Struct.* **2016**, *111*, 323–332.

25. Yoo, D.-Y.; Yuan, T.; Yang, J.-M.; Yoon, Y.-S. Feasibility of replacing minimum shear reinforcement with steel fibers for sustainable high-strength concrete beams. *Eng. Struct.* **2017**, *147*, 207–232.

26. Ranjan, S.D.; Abhimanyu, S. Effect of steel fiber content on behavior of concrete beams with and without stirrups. *ACI Struct. J.* **2014**, *111*, 1157–1166.

27. Kim, C.-G.; Lee, H.; Park, H.-G.; Hong, G.-H.; Kang, S.-M. Effect of Steel Fibers on Minimum Shear Reinforcement of High-Strength Concrete Beams. *ACI Struct. J.* **2017**, *114*, 1109–1119. [CrossRef]

28. Aoude, H.; Belghiti, M.; Cook, W.D.; Mitchell, D. Response of Steel Fiber-Reinforced Concrete Beams with and without Stirrups. *ACI Struct. J.* **2012**, *109*, 359–367. [CrossRef]

29. Yoo, D.-Y.; Yang, J.-M. Effects of stirrup, steel fiber, and beam size on shear behavior of high-strength concrete beams. *Cem. Concr. Compos.* **2018**, *87*, 137–148. [CrossRef]

30. Di Prisco, M.; Romero, J.A. Diagonal shear in thin-webbed reinforced concrete beams: Fibre and stirrup roles at shear collapse. *Mag. Concr. Res.* **1996**, *48*, 59–76. [CrossRef]

31. Zhao, J.; Liang, J.; Chu, L.; Shen, F. Experimental Study on Shear Behavior of Steel Fiber Reinforced Concrete Beams with High-Strength Reinforcement. *Materials* **2018**, *11*, 1682. [CrossRef] [PubMed]

32. Biolzi, L.; Cattaneo, S. Response of steel fiber reinforced high strength concrete beams: Experiments and code predictions. *Cem. Concr. Compos.* **2017**, *77*, 1–13. [CrossRef]

33. Junior, S.F.; De Hanai, J.B. Shear behavior of fiber reinforced concrete beams. *Cem. Concr. Compos.* **1997**, *19*, 359–366.

34. Turmo, J.; Banthia, N.; Gettu, R.; Barragán, B. Study of the shear behaviour of fibre reinforced concrete beams. *Mater. Constr.* **2008**, *58*, 5–13.

35. Campione, G. Flexural and Shear Resistance of Steel Fiber–Reinforced Lightweight Concrete Beams. *J. Struct. Eng.* **2014**, *140*, 04013103. [CrossRef]

36. Li, C.Y.; Liang, N.; Zhao, M.L.; Yao, K.Q.; Li, J.; Li, X.K. Shear Performance of Reinforced Concrete Beams Affected by Satisfactory Composite-Recycled Aggregates. *Materials* **2020**, *13*, 1711. [CrossRef] [PubMed]

37. Ministry of Housing and Urban-Rural Development of the People's Republic of China. *Technical Specification for Lightweight-Aggregate Concrete Structures*; JGJ12-2006; China Building Industry Press: Beijing, China, 2006.

38. Ministry of Housing and Urban-Rural Development of the People's Republic of China. *Code for Design of Concrete Structures*; GB50010-2010; China Building Industry Press: Beijing, China, 2010.
39. Ministry of Housing and Urban-Rural Development of the People's Republic of China. *Standard for Design of Steel Fiber Reinforced Concrete Structures*; JGJ/T465-2019; China Building Industry Press: Beijing, China, 2020.
40. Ministry of Housing and Urban-Rural Development of the People's Republic of China. *Steel Fiber Reinforced Concrete*; JG/T472-2015; China Building Industry Press: Beijing, China, 2015.
41. Canadian Standards Association. *Design of Concrete Structures: Structures Design*; CSA A23.3-04; Canadian Standards Association: Mississauga, TN, Canada, 2004.
42. British Standards Institution. *Design of Concrete Structures: Part 1-1: General Rules and Rules for Buildings*; Eurocode 2; British Standards Institution: London, UK, 2004.
43. ACI Committee 318. *Building Code Requirements for Structural Concrete*; ACI 318-14; ACI: Farmington Hill, MI, USA, 2014.
44. ACI Committee 544. *Design Considerations for Steel Fiber Reinforced Concrete*; ACI 544.4R-2009; ACI: Farmington Hill, MI, USA, 2009.